

Long-Range Resonance Energy Transfer to $[\text{Ru}(\text{bpy})_3]^{2+}$

Daniel S. Tyson,[‡] Ignacy Gryczynski,[†] and Felix N. Castellano^{*,‡}

Department of Chemistry and Center for Photochemical Sciences, Bowling Green State University, Bowling Green, Ohio 43403, and Center for Fluorescence Spectroscopy, University of Maryland School of Medicine, Baltimore, Maryland 21201

Received: November 12, 1999; In Final Form: January 25, 2000

We report the first experimental evidence of long-range nonradiative singlet–singlet resonance energy transfer from excited coumarin 460 molecules to $[\text{Ru}(\text{bpy})_3]^{2+}$ acceptors (bpy is 2,2'-bipyridine). The molecules were randomly dispersed in fluid solutions of both high (glycerol) and low (CH_3CN) viscosity at room temperature. The frequency-domain donor (coumarin 460) fluorescence decays were satisfactorily analyzed in terms of Förster theory incorporating a term for translational diffusion. Two different $[\text{Ru}(\text{bpy})_3]^{2+}$ (quencher) concentrations in each solvent were used, and the coumarin 460 emission was measured and analyzed both independently and globally. In glycerol, diffusion does not play a significant role in the energy transfer process, whereas in CH_3CN , diffusion is able to enhance the energy transfer reaction. In both solvents, mutual diffusion coefficients were determined from the experimental data and χ^2_{R} error surfaces were constructed to judge their statistical uncertainty. The results demonstrate that metal-to-ligand charge transfer compounds can serve as intermolecular energy transfer acceptors in schemes utilizing long-range Förster-type processes.

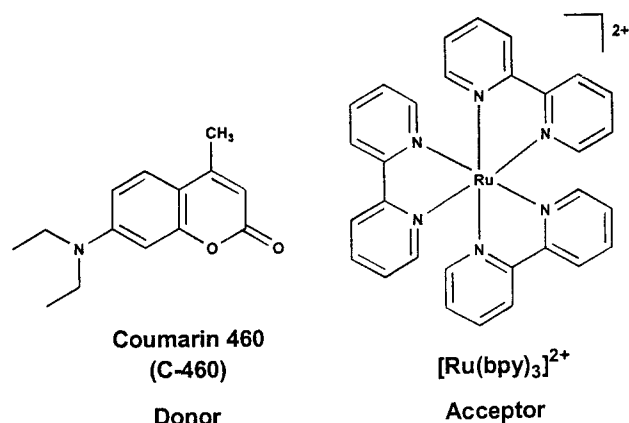
Introduction

Förster-type singlet–singlet energy transfer processes govern the efficient capture and funneling of photonic energy in the primary steps of natural photosynthesis.^{1,2} Such resonance energy transfer (RET) processes are modulated by several factors, including donor–acceptor orientation, distance, and spectral overlap.^{1–6} These properties have been exploited in the design of numerous light-harvesting molecules and artificial photosynthetic assemblies.^{7–15} There are also several examples where RET has been used as a molecular ruler in various biological systems.^{6,16,17}

In previous studies, our group¹⁸ and others^{19–21} have shown that intramolecular singlet energy transfer from organic chromophores to metal-to-ligand charge transfer (MLCT) compounds²² occurs both rapidly and efficiently. In each supramolecular array, characteristic long-lived MLCT emission is sensitized through the excitation of the pendant organic pigments. Since the chromophores are in relatively close contact in such arrangements, singlet energy transfer may occur by two mechanisms: the dipole–dipole Förster mechanism^{2–6} or the electron exchange Dexter mechanism.²³ The two processes are typically distinguished by evaluating the energy transfer rate as a function of donor–acceptor separation distance, inevitably requiring copious amounts of synthesis. To date, the supramolecular MLCT-based systems described above have not established the operational singlet energy transfer mechanism. The current work seeks to verify the existence of the Förster mechanism using $[\text{Ru}(\text{bpy})_3]^{2+}$ (bpy is 2,2'-bipyridine), the benchmark MLCT chromophore, as energy acceptors. In previous related work, Demas and co-workers investigated the opposite reaction: intermolecular singlet energy transfer from the MLCT excited states of $[\text{Ru}(\text{bpy})_3]^{2+}$ to a variety of laser

dyes.²⁴ This classic study strongly supported the spin–orbit model proposed by Crosby et al. for the charge transfer states of platinum metal compounds.²⁵

In an effort to probe the mechanism of singlet energy transfer from organic pigments to Ru(II) MLCT complexes, we turned to intermolecular systems. This is a logical choice, as there exists both a theoretical foundation and analytical expressions for intermolecular RET processes.^{26–31} Three-dimensional solutions of randomly distributed donors and acceptors can be studied under conditions where the donor and acceptor are separated by large distances (on average), and the quenched donor fluorescence or the sensitized acceptor emission can be quantitatively analyzed. In the present study we use coumarin 460 (C-460) as an energy transfer donor for $[\text{Ru}(\text{bpy})_3]^{2+}$. Förster-



type energy transfer is likely to occur in this system due to the large spectral overlap between the C-460 emission spectrum and the $[\text{Ru}(\text{bpy})_3]^{2+}$ absorption spectrum. The energy transfer is conveniently monitored by the lifetime quenching of the C-460 emission and is found to be consistent with a long-range Förster mechanism.

* Address correspondence to this author. E-mail: castell@bgnet.bgsu.edu.

[‡] Bowling Green State University.

[†] Center for Fluorescence Spectroscopy.

Experimental Section

General Comments. Glycerol, [Ru(bpy)₃]Cl₂, and spectroscopic grade CH₃CN were obtained from Aldrich and used as received. [Ru(bpy)₃](PF₆)₂ was available from previous studies.¹⁸ 7-Diethylamino-4-methylcoumarin (Coumarin 460, C-460) was purchased from Exciton and used as received. All other reagents and materials from commercial sources were used as received.

Physical Measurements. Absorption spectra were measured with a Hewlett-Packard 8453 diode array spectrophotometer, accurate to ±2 nm. The instrument used to measure static luminescence spectra was described previously.^{18b} Luminescence excitation and emission spectra were measured in 1 mm path length quartz optical cells. Preliminary fluorescence lifetime measurements used a commercially available time-correlated single-photon-counting apparatus (Edinburgh Instruments) equipped with a H₂ nanosecond flashlamp excitation source.^{18b}

The quantum yields of C-460 in glycerol and CH₃CN were obtained from the literature and are 0.58 and 1.0, respectively.³² The refractive indexes of glycerol and CH₃CN used in the calculation of Förster distances are 1.475 and 1.34, respectively. The concentration of C-460 (donor) was maintained at 10⁻⁴ M in all experiments unless otherwise stated. At this concentration, the fluorescence intensity decays are single exponential in glycerol and CH₃CN, in quantitative agreement with literature values.³² In all cases, the absorption spectra of C-460/[Ru(bpy)₃]²⁺ mixtures were the sum of that found for the two individual chromophores, suggesting that there is no ground-state association under our experimental conditions.

Fluorescence intensity decay measurements were performed using front-face geometry with samples maintained at 20 ± 1 °C. Frequency-domain fluorescence lifetime measurements were performed using an instrument described previously.³³ Briefly, the modulated excitation was provided by the harmonic content of a 3.76 MHz train of 5 ps pulses from a cavity-dumped Pyridine-2 dye laser synchronously pumped by a mode-locked argon ion laser (Coherent). The dye laser output was frequency doubled to 370 nm using a Spectra Physics Model 390 doubler and used to excite the samples. The emission detector was a microchannel plate photomultiplier (MCP-PMT, Hamamatsu R1564U). Prior to the MCP-PMT, the C-460 emission was passed through a 470 ± 20 nm interference filter, using magic angle polarizer conditions. For all analyses the uncertainties in the phase (δ_φ) and modulation (δ_m) measurements were 0.3 and 0.007, respectively. In all frequency-domain measurements the optical densities of the reference and sample were matched to equalize the optical path lengths. Data analysis was accomplished with nonlinear least-squares software that was developed in the Center for Fluorescence Spectroscopy, using the models described below.^{31,34,35} In some cases, multiple decay curves were globally analyzed.

Theory

There are several theories that describe fluorescence intensity decays in the presence of resonance energy transfer.²⁶⁻²⁹ Here we consider the case for donors and acceptors randomly distributed in homogeneous solution in three dimensions. Under our experimental conditions, the intensity decay of the donor, $I_D(t)$, is single exponential in the absence of acceptor,

$$I_D(t) = I_D^0 \exp\left(-\frac{t}{\tau_D^0}\right) \quad (1)$$

where τ_D^0 is the decay time of the donor and t is time. In cases where resonance energy transfer occurs to randomly distributed

acceptors, the donor fluorescence decays nonexponentially according to the Förster relation²

$$I_D(t) = I_D^0 \exp\left[-\frac{t}{\tau_D^0} - 2\gamma\left(\frac{t}{\tau_D^0}\right)^{1/2}\right] \quad (2)$$

where $\gamma = C_A/C_A^0$, C_A is the molar concentration of the acceptor, and C_A^0 is the molar critical concentration.

$$C_A^0 = \frac{3000}{2\pi^{3/2}NR_0^3} \quad (3)$$

Here N is Avogadro's number and R_0 is the critical transfer distance given by Förster, eq 4.²

$$R_0^6 = \frac{9000(\ln 10)\kappa^2\phi_D^0}{128\pi^5N\eta^4} \int_0^\infty F_D(\lambda) \epsilon_A(\lambda)\lambda^4 d\lambda \quad (4)$$

κ^2 is the orientation factor, ϕ_D^0 is the fluorescence quantum yield of the donor in the absence of acceptor, η is the refractive index of the solvent, $F_D(\lambda)$ is the emission spectrum of the donor with the area normalized to unity, $\epsilon_A(\lambda)$ is the absorption spectrum of the acceptor in units of M⁻¹ cm⁻¹, and λ is the wavelength in nanometers. In the present work κ^2 is equated to 2/3, assuming random donor-acceptor orientations during the energy transfer event. As can be inferred, the Förster distance, R_0 , is readily calculated from the spectral properties of the donor and acceptor. Using C-460 as a donor and [Ru(bpy)₃]²⁺ as an acceptor, R_0 values calculated from eq 4 are 37.7 and 44 Å in glycerol and CH₃CN, respectively.

Förster theory works well for donors and acceptors dissolved in solvents of high viscosity, where little or no diffusion is permissible. However, in solvents of low viscosity at room temperature, resonance energy transfer is enhanced by diffusion. Yokota and Tanimoto used an approximation method to evaluate an exact expression for Förster transfer in a fluid medium with significant diffusion, eq 5.²⁸

$$I_D(t) = I_D^0 \exp\left[-\frac{t}{\tau_D^0} - 2B\gamma\left(\frac{t}{\tau_D^0}\right)^{1/2}\right] \quad (5)$$

Gösele and co-workers later proposed an improved formulation²⁹⁻³¹ that properly accounts for the energy transfer rate in the longer time regime using a different B parameter, eq 6,

$$B = \left(\frac{1 + 5.47x + 4x^2}{1 + 3.34x}\right)^{3/4} \quad (6)$$

which is related to the diffusional and energy transfer processes by

$$x = D\beta^{-1/3}t^{2/3} \quad \beta = \frac{R_0^6}{\tau_D^0} \quad (7)$$

where D is the diffusion coefficient. When diffusion does not influence the energy transfer rate, $B = 1$, and eq 5 reduces to the Förster relationship, eq 2. In the energy transfer data analysis, D and/or R_0 will be floating parameters, while the other parameters remain fixed.

The frequency response of the emission, characterized by the frequency (ω)-dependent values of the phase shift (ϕ_ω) and extent of demodulation (m_ω), is related directly to any emission decay law.^{6,31,34,35} The parameters describing the decay law are compared with the calculated values of phase and modulation.

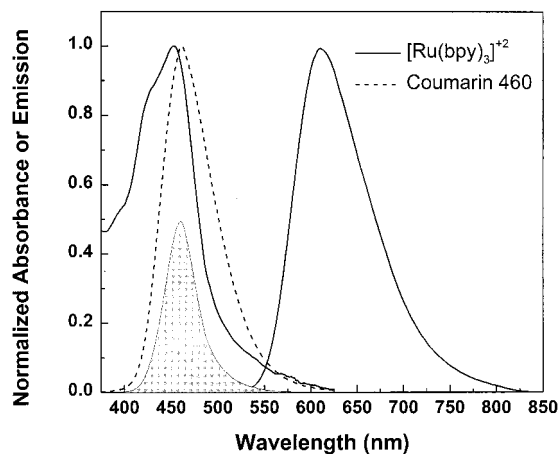


Figure 1. Absorption and emission spectrum of $[\text{Ru}(\text{bpy})_3]^{2+}$ (solid lines) and emission spectrum of C-460 (dashed line) in CH_3CN . The shaded area represents the spectral overlap of the two chromophores.

The goodness-of-fit is characterized by χ^2_{R} and by visual inspection of the phase and modulation residuals.

Results and Discussion

The emission spectrum of C-460 and the absorption and emission spectra of $[\text{Ru}(\text{bpy})_3]^{2+}$ in CH_3CN at room temperature are displayed in Figure 1. Superimposed on this plot is a representation of the substantial spectral overlap ($J = 4.06 \times 10^{-14} \text{ M}^{-1} \text{ cm}^3$ (CH_3CN), $J = 4.04 \times 10^{-14} \text{ M}^{-1} \text{ cm}^3$ (glycerol)) of the two chromophores. Importantly, the emission spectra of the two compounds are well separated, allowing selective monitoring of the C-460 fluorescence. Concentrations of $[\text{Ru}(\text{bpy})_3]^{2+}$ from 2.5 to 10 mM quench the C-460 fluorescence in both glycerol and CH_3CN . It should be noted that the average center-to-center distance (r_{av} , in Å) between the donor and acceptor can be estimated with eq 8:³⁶

$$r_{\text{av}} = \left(\frac{3 \times 10^{27}}{4\pi[A]N} \right)^{1/3} \quad (8)$$

where $[A]$ is the molar concentration of the acceptor (C-460). At 2.5 mM, the average separation distance is 54 Å, and at 10 mM, this separation shortens to 34 Å. In conjunction with a short-lifetime fluorophore, long-range interactions are largely favored over short-range collisional processes under these experimental conditions. In the pure solvents without acceptor, C-460 displays single-exponential fluorescence decays with lifetimes of 3.69 and 3.31 ns in glycerol and CH_3CN , respectively.

In an effort to demonstrate that C-460 sensitizes the charge-transfer-based emission in $[\text{Ru}(\text{bpy})_3]^{2+}$, we measured corrected excitation spectra of equimolar mixtures of the two species in CH_3CN . Figure 2 represents a typical set of data where the emission of $[\text{Ru}(\text{bpy})_3]^{2+}$ is monitored at $650 \pm 1 \text{ nm}$ in mixtures of the two chromophores. Samples containing only $[\text{Ru}(\text{bpy})_3]^{2+}$ and C-460 were measured under identical conditions for comparison. The corrected excitation spectra are normalized to unity at the peak of the MLCT transition in the visible, where only $[\text{Ru}(\text{bpy})_3]^{2+}$ appreciably absorbs. In the absence of energy transfer from C-460 to $[\text{Ru}(\text{bpy})_3]^{2+}$, the excitation spectrum would match that of $[\text{Ru}(\text{bpy})_3]^{2+}$ alone (Figure 2, dotted line). Clearly, the excitation spectrum of the mixture in Figure 2 (solid line) includes contributions additional to that resulting from direct excitation of $[\text{Ru}(\text{bpy})_3]^{2+}$ at short wavelengths, suggesting that C-460 sensitizes the MLCT

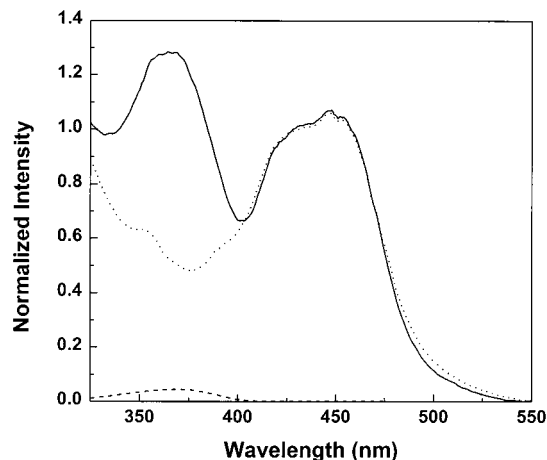


Figure 2. Corrected photoluminescence excitation spectra of $[\text{Ru}(\text{bpy})_3]^{2+}$ (dotted line), C-460 (dashed line), and an equimolar mixture of C-460 and $[\text{Ru}(\text{bpy})_3]^{2+}$ (solid line) in CH_3CN at 20 °C. Samples (0.5 mM) were contained in a 1 mm path length quartz optical cell, and emission was monitored at $650 \pm 1 \text{ nm}$.

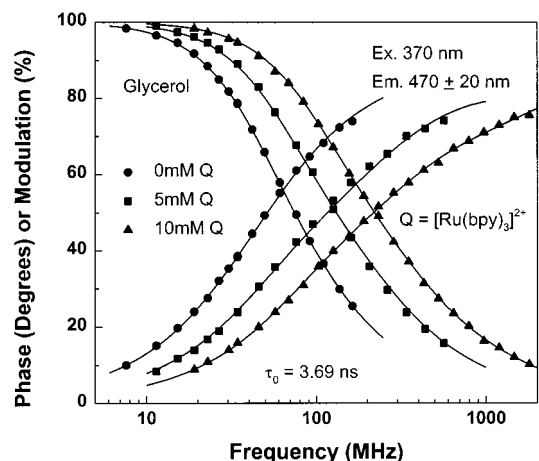


Figure 3. Frequency-domain C-460 intensity decays in the absence (filled circles) and in the presence of 5 mM (filled squares) and 10 mM (filled triangles) $[\text{Ru}(\text{bpy})_3]^{2+}$ in glycerol at 20 °C. The samples were excited with pulsed excitation at 370 nm (5 ps fwhm, 3.76 MHz), and emission was detected through a $470 \pm 20 \text{ nm}$ interference filter. In the absence of quencher, the solid lines are the best fit to the single-exponential model (eq 1). In the presence of quencher (5 and 10 mM), the solid lines are the best fits to the Gösele model (eqs 5 and 6).

emission. Under these particular experimental conditions, some residual C-460 fluorescence contributes minimally to the total intensity at 650 nm (Figure 2, dashed line). However, this minor component does not account for the majority of the sensitized emission detected. Additional evidence of the sensitization is derived from the observation of increasing energy transfer efficiency with increasing $[\text{Ru}(\text{bpy})_3]^{2+}$ concentration (data not shown). In these studies, excitation spectra of equimolar mixtures of $[\text{Ru}(\text{bpy})_3]^{2+}$ and C-460 in CH_3CN were analyzed as described by Demas and co-workers.^{24c} Although the steady-state data illustrates the sensitization process, detailed analysis requires substantial manipulation to correct for inner-filter effects at the high concentrations of acceptor necessary. Therefore, time-resolved measurements were performed, allowing direct measurement of the C-460 intensity decays in the presence and absence of singlet energy transfer to $[\text{Ru}(\text{bpy})_3]^{2+}$.

Frequency-domain data for the intensity decay of C-460 emission in the absence and in the presence of 5 and 10 mM $[\text{Ru}(\text{bpy})_3]^{2+}$ in glycerol are presented in Figure 3. In the presence of randomly distributed acceptors the decay becomes

TABLE 1: Recovered C-460 Decay Parameters and Donor-to-Acceptor Diffusion Coefficients at 20 °C^a

solvent	[Ru(bpy) ₃] ²⁺ (mM)	decay model ^b	τ_D (ns)	R_0 (Å) ^c	D (cm ² s ⁻¹)	χ^2_R
glycerol	0	1 exp	3.69			1.05
	5	1 exp	1.81			109.19
	10	1 exp	0.964			261.74
	5	Gösele	$\langle 3.69 \rangle$	$\langle 37.7 \rangle$	4.05×10^{-7}	1.03
	5	Gösele	$\langle 3.69 \rangle$	38	7.41×10^{-8}	0.97
	10	Gösele	$\langle 3.69 \rangle$	$\langle 37.7 \rangle$	6.08×10^{-7}	0.94
	10	Gösele	$\langle 3.69 \rangle$	38	1.1×10^{-7}	0.74
	5 and 10	Gösele (global) ^d	$\langle 3.69 \rangle$	$\langle 37.7 \rangle$	5.3×10^{-7}	0.99
	5 and 10	Gösele (global) ^d	$\langle 3.69 \rangle$	38	7.45×10^{-8}	0.82
	CH ₃ CN	0	1 exp	3.31		
2.5		1 exp	1.37			42.9
5		1 exp	0.744			113.56
2.5		Gösele	$\langle 3.31 \rangle$	$\langle 44 \rangle$	3.1×10^{-5}	0.87
2.5		Gösele	$\langle 3.31 \rangle$	43.8	3.2×10^{-5}	0.89
5		Gösele	$\langle 3.31 \rangle$	$\langle 44 \rangle$	3.17×10^{-5}	1.53
5		Gösele	$\langle 3.31 \rangle$	44.4	2.9×10^{-5}	1.45
2.5 and 5		Gösele (global) ^d	$\langle 3.31 \rangle$	$\langle 44 \rangle$	3.1×10^{-5}	1.25
2.5 and 5		Gösele (global) ^d	$\langle 3.31 \rangle$	44.3	2.95×10^{-5}	1.21

^a $\langle \rangle$ indicates that the parameter was held fixed during the data analysis. ^b 1 exp represents a single-exponential fit, eq 1; Gösele represents the Förster model with diffusion, eq 5. ^c The fixed Förster distances were calculated from the spectral properties of C-460 and [Ru(bpy)₃]²⁺. ^d Global represents the best fit from simultaneous analysis of both sets of quenching decay curves.

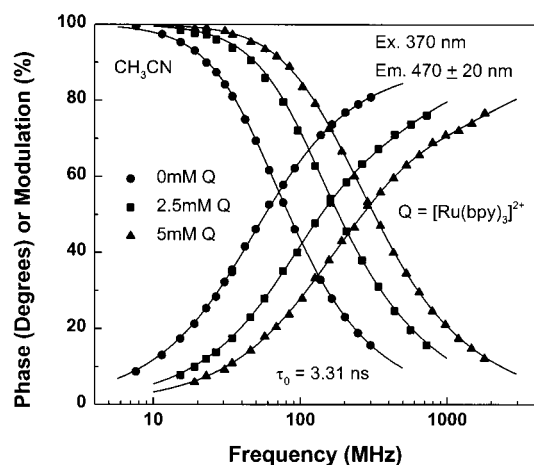


Figure 4. Frequency-domain C-460 intensity decays in the absence (filled circles) and in the presence of 2.5 mM (filled squares) and 5 mM (filled triangles) [Ru(bpy)₃]²⁺ in CH₃CN at 20 °C. The samples were excited with pulsed excitation at 370 nm (5 ps fwhm, 3.76 MHz), and emission was detected through a 470 ± 20 nm interference filter. In the absence of quencher, the solid lines are the best fit to the single-exponential model (eq 1). In the presence of quencher (2.5 and 5 mM), the solid lines are the best fits to the Gösele model (eqs 5 and 6).

heterogeneous compared to that in the absence of acceptors. The origin of the heterogeneity is derived from a distribution of donor–acceptor distances, leading to a range of transfer rates. The data with 5 and 10 mM [Ru(bpy)₃]²⁺ could not be adequately modeled with a single-exponential fit (Table 1), nor could it be modeled with a sum of two exponentials (data not shown). Each set of quenching data could be modeled using the Gösele model, eqs 5 and 6. As can be inferred from the analysis (Table 1), the Förster equation (eq 2) also provides an adequate representation of the data given the extremely small value of the recovered diffusion coefficients (10^{-7} – 10^{-8} cm² s⁻¹). These results suggest that the donor–acceptor distribution in the highly viscous solvent glycerol (1412 cP)³⁷ is quite stationary during the energy transfer event.

Figure 4 displays the frequency-domain fluorescence decays of C-460 in the absence and presence of 2.5 and 5.0 mM [Ru(bpy)₃]²⁺ in CH₃CN. In these cases, the samples containing quencher display heterogeneous kinetics that could not be adequately modeled with a single-exponential fit (Table 1) or

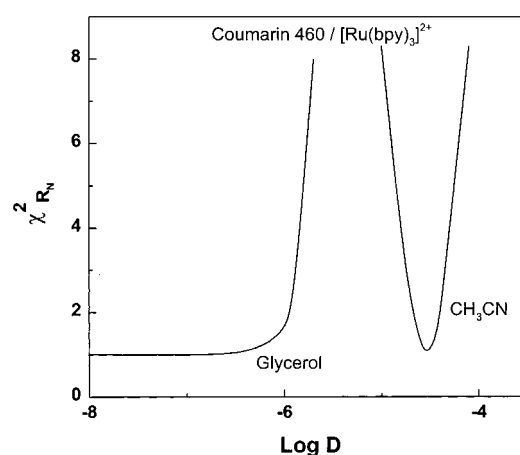


Figure 5. Dependence of χ^2_R on the diffusion coefficients recovered from the Gösele model in glycerol and CH₃CN.

the Förster model without diffusion (data not shown). Both sets of data, however, could be adequately represented with the Gösele model (Table 1) that accounts for diffusional enhancement of Förster-type energy transfer in fluidic nonrigid solvents. The diffusion coefficients in CH₃CN recovered from least-squares analysis using the Gösele model (Table 1) are consistent with the low viscosity of this solvent (0.35 cP).

The uncertainties in the diffusion coefficients can be judged through examination of the χ^2_R surfaces, Figure 5.^{6,31} These surfaces were calculated by holding the diffusion coefficient (D) fixed at the values indicated on the x -axis and allowing R_0 to vary so as to minimize χ^2_R . This clearly provides the worst case scenario for analysis because R_0 is known from the spectral data of the two chromophores. In fact if R_0 is maintained fixed during the analysis using that calculated from the spectral data, the values of D become known with greater certainty (data not shown). In the case of glycerol, values of D less than 4×10^{-7} cm² s⁻¹ fit the data with equal statistical certainty. This result suggests that translational diffusion does not affect the energy transfer reaction in glycerol. Clearly the χ^2_R surface is much steeper in CH₃CN, indicating the influence of diffusion on the energy transfer process. Here, the global minimum was determined to be 2.95×10^{-5} cm² s⁻¹, which is reasonable in light of the low viscosity of CH₃CN and the molecular dimensions of the chromophores.³⁸

The highly efficient quenching of the C-460 emission by [Ru(bpy)₃]²⁺ is consistent with a long-range Förster RET mechanism. The rate of intermolecular energy transfer in the Dexter mechanism is proportional to the orbital overlap, attenuating exponentially with distance. Such a short-range mechanism would quench all excited molecules within a few angstroms and have no quenching effect on the remaining excited volume. In all cases the lifetime quenching data using multiexponential models failed to recover any lifetimes near or equal to τ_0 , indicative of a predominant long-range mechanism. Although electron exchange energy transfer cannot be completely ruled out as a competing mechanism, we believe its effects are largely minimized under the experimental conditions used in the time-resolved measurements. The heterogeneity of the C-460 intensity decays in the presence of [Ru(bpy)₃]²⁺ is consistent with Förster-type transfer. The Förster kinetic models also represent the data with good statistical certainty. In the worst cases, the analysis required only two variable parameters, even when two sets of quenching data were globally analyzed. Under circumstances where R_0 is floated in the data analysis, the recovered values are in surprisingly good agreement with that calculated from the spectral properties of the two chromophores, Table 1. Further evidence of Förster-type transfer comes from the recovered diffusion coefficients. In glycerol, diffusion has little or no effect on the transfer and the data can be modeled using eq 2 with one variable parameter (R_0). In CH₃CN, diffusion enhances the energy transfer consistent with the Gösele model (Förster with translational diffusion). Analysis of the CH₃CN data recovered the same mutual diffusion coefficient, whose value is representative of that expected for a low-viscosity solvent.

Conclusions

In the present work, Ru(II) MLCT excited states are sensitized by excitation of C-460 molecules through intermolecular singlet–singlet energy transfer processes. The data provide good evidence that Förster-type transfer dominates C-460 quenching by [Ru(bpy)₃]²⁺. Since C-460 has substantial absorption near the onset of the visible (350–400 nm), it acts as an intermolecular light-harvesting antenna for the redox-active [Ru(bpy)₃]²⁺, which possesses small absorption cross sections over this wavelength range. In addition, the short-lived C-460 is converted into a long-lived MLCT excited state capable of further intermolecular energy or electron transfer chemistry. The ability to access MLCT excited states with long-range intermolecular RET has potential applications in light-conversion molecular devices.^{13,14} Demanding synthetic procedures are minimized if intermolecular processes are substituted for covalently linked intramolecular assemblies. Recently, intermolecular light-harvesting arrays have been applied in the design of an artificial inorganic “leaf” using a polyelectrolyte self-assembly approach.¹⁵ This arrangement utilized Pd(II) porphyrin redox “trap” molecules as the final energy transfer acceptors. The present work demonstrates that MLCT compounds are also viable chromophores for incorporation into related artificial photosynthetic assemblies.

Acknowledgment. We would like to thank a reviewer for suggesting the inclusion of the sensitization data.

References and Notes

- (1) *Photosynthetic Light-Harvesting Systems*; Scheer, H., Siegried, S., Eds.; Walter de Gruyter: New York, 1988.
- (2) (a) Förster, T. *Ann. Phys. (Leipzig)* **1948**, *2*, 55. (b) Förster, T. *Z. Naturforsch.* **1949**, *4a*, 321. (c) Förster, T. *Discuss. Faraday Soc.* **1959**, *27*, 7.

- (3) Latt, S. A.; Cheung, H. T.; Blout, E. R. *J. Am. Chem. Soc.* **1965**, *87*, 995.
- (4) (a) Stryer, L.; Haugland, R. P. *Proc. Natl. Acad. Sci.* **1967**, *58*, 719. (b) Haugland, R. P.; Yguerabide, J.; Stryer, L. *Proc. Natl. Acad. Sci.* **1969**, *63*, 23.
- (5) Dale, R. E.; Eisinger, J. *Biopolymers* **1974**, *13*, 1573.
- (6) Lakowicz, J. R. *Principles of Fluorescence Spectroscopy*, 2nd ed.; Kluwer Academic/Plenum Publishers: New York, 1999.
- (7) (a) Gust, D.; Moore, T. A.; Moore, A. L. *Acc. Chem. Res.* **1993**, *26*, 198. (b) Moore, T. A.; Gust, D.; Moore, A. L. *Pure Appl. Chem.* **1994**, *66*, 1033. (c) Steinberg-Yfrach, G.; Liddell, P. A.; Hung, S. C.; Moore, A. L.; Gust, D.; Moore, T. A. *Nature* **1997**, *385*, 239. (d) Steinberg-Yfrach, G.; Rigaud, J. L.; Durantini, E. N.; Moore, A. L.; Gust, D.; Moore, T. A. *Nature* **1998**, *392*, 479.
- (8) (a) Prathapan, S.; Johnson, T. E.; Lindsey, J. S. *J. Am. Chem. Soc.* **1993**, *115*, 7519. (b) Wagner, R. W.; Lindsey, J. S. *J. Am. Chem. Soc.* **1994**, *116*, 9759. (c) Wagner, R. W.; Lindsey, J. S. *Pure Appl. Chem.* **1996**, *68*, 1373. (d) Li, F.; Yang, S. I.; Ciringhy, Y.; Seth, J.; Martin, C. H.; Singh, D. L.; Kim, D.; Birge, R. R.; Bocian, D. F.; Holten, D.; Lindsey, J. S. *J. Am. Chem. Soc.* **1998**, *120*, 10001.
- (9) (a) Fox, M. A. *Acc. Chem. Res.* **1992**, *25*, 569. (b) Watkins, D. M.; Fox, M. A. *J. Am. Chem. Soc.* **1994**, *116*, 6441. (c) Stewart, G. M.; Fox, M. A. *J. Am. Chem. Soc.* **1996**, *118*, 4354.
- (10) (a) Devadoss, C.; Bharathi, P.; Moore, J. S. *J. Am. Chem. Soc.* **1996**, *118*, 9635. (b) Shortreed, M. R.; Swallen, S. F.; Shi, Z. Y.; Tan, W.; Xu, Z.; Devadoss, C.; Moore, J. S.; Kopelman, R. *J. Phys. Chem. B* **1997**, *101*, 6318.
- (11) (a) Gilat, S. L.; Adronov, A.; Fréchet, J. M. *J. Angew. Chem., Int. Ed.* **1999**, *38*, 1422. (b) Gilat, S. L.; Adronov, A.; Fréchet, J. M. *J. Org. Chem.* **1999**, *64*, 7474.
- (12) (a) Jiang, D.-L.; Aida, T. *J. Am. Chem. Soc.* **1998**, *120*, 10895. (b) Sato, T.; Jiang, D.-L.; Aida, T. *J. Am. Chem. Soc.* **1999**, *121*, 10658.
- (13) (a) Balzani, V.; Juris, A.; Venturi, M.; Campagna, S.; Serroni, S. *Chem. Rev.* **1996**, *96*, 759, and references therein. (b) Balzani, V.; Scandola, F. *Supramolecular Photochemistry*; Horwood: Chichester, 1991.
- (14) Lehn, J.-M. *Supramolecular Chemistry: Concepts and Perspectives*; VCH: Weinheim, 1995, and references therein.
- (15) Kaschak, D. M.; Lean, J. T.; Waraksa, C. C.; Saupe, G. B.; Usami, H.; Mallouk, T. E. *J. Am. Chem. Soc.* **1999**, *121*, 3435.
- (16) Stryer, L. *Annu. Rev. Biochem.* **1978**, *47*, 819.
- (17) Wu, P.; Brand, L. *Anal. Biochem.* **1994**, *218*, 1.
- (18) (a) Tyson, D. S.; Castellano, F. N. *Inorg. Chem.* **1999**, *38*, 4382. (b) Tyson, D. S.; Castellano, F. N. *J. Phys. Chem. A* **1999**, *103*, 10955.
- (19) (a) Wilson, G. J.; A.; Sasse, W. H. F.; Mau, A. W. H. *Chem. Phys. Lett.* **1996**, *250*, 583. (b) Wilson, G. J.; Launikonis, A.; Sasse, W. H. F.; Mau, A. W. H. *J. Phys. Chem. A* **1997**, *101*, 4860. (c) Wilson, G. J.; Launikonis, A.; Sasse, W. H. F.; Mau, A. W. H. *J. Phys. Chem. A* **1998**, *102*, 5150.
- (20) (a) Plevovets, M.; Vögtle, F.; De Cola, L.; Balzani, V. *New J. Chem.* **1999**, *23*, 63. (b) Schlicke, B.; Belser, P.; De Cola, L.; Sabbioni, E.; Balzani, V. *J. Am. Chem. Soc.* **1999**, *121*, 4207.
- (21) Ley, K. D.; Whittle, C. E.; Bartberger, M. D.; Schanze, K. S. *J. Am. Chem. Soc.* **1997**, *119*, 3423.
- (22) For reviews of MLCT excited states: (a) Juris, A.; Balzani, V.; Barigelli, F.; Campagna, S.; Belser, P.; von Zelewsky, A. *Coord. Chem. Rev.* **1988**, *84*, 85. (b) Meyer, T. *J. Acc. Chem. Res.* **1989**, *22*, 1048. (c) Demas, J. N.; DeGraff, B. A. *Anal. Chem.* **1991**, *63*, 829A. (d) Kalyanasundaram, K. *Photochemistry of Polypyridine and Porphyrin Complexes*; Academic Press: San Diego, 1992. (e) Roundhill, D. M. *Photochemistry and Photophysics of Metal Complexes*; Plenum Press: New York, 1994. (f) Ramamurthy, V.; Schanze, K. S., Eds. *Organic and Inorganic Photochemistry*; M. Dekker: New York, 1998.
- (23) Dexter, D. L. *J. Chem. Phys.* **1953**, *21*, 836.
- (24) (a) Mandal, K.; Pearson, T. D. L.; Demas, J. N. *J. Chem. Phys.* **1980**, *73*, 2507. (b) Mandal, K.; Demas, J. N. *Chem. Phys. Lett.* **1981**, *84*, 410. (c) Mandal, K.; Pearson, T. D. L.; Krug, W. P.; Demas, J. N. *J. Am. Chem. Soc.* **1983**, *105*, 701.
- (25) (a) Hager, G. D.; Crosby, G. A. *J. Am. Chem. Soc.* **1975**, *97*, 7031. (b) Hager, G. D.; Watts, R. J.; Crosby, G. A. *J. Am. Chem. Soc.* **1975**, *97*, 7037. (c) Hipps, K. W.; Crosby, G. A. *J. Am. Chem. Soc.* **1975**, *97*, 7042. (d) Elfring, W. H.; Crosby, G. A. *J. Am. Chem. Soc.* **1981**, *103*, 2683.
- (26) Bennett, R. G. *J. Chem. Phys.* **1964**, *41*, 3037.
- (27) Birks, J. B.; Georghiou, S. *J. Phys. Soc. B* **1968**, *1*, 958.
- (28) Yokota, M.; Tanimoto, O. *J. Phys. Soc. Jpn.* **1967**, *22*, 779.
- (29) Gösele, U.; Hauser, M.; Klein, U. K. A.; Frey, R. *Chem. Phys. Lett.* **1975**, *34*, 519.
- (30) Millar, D. P.; Robbins, R. J.; Zewail, A. H. *J. Chem. Phys.* **1981**, *75*, 3649.
- (31) Lakowicz, J. R.; Szmecinski, H.; Gryczynski, I.; Wicz, W.; Johnson, M. L. *J. Phys. Chem.* **1990**, *94*, 8413.

(32) Jones, G., II; Jackson, W. R.; Choi, C. Y.; Bergmark, W. R. *J. Phys. Chem.* **1985**, *89*, 294.

(33) Lakowicz, J. R.; Laczko, G.; Gryczynski, I. *Rev. Sci. Instrum.* **1986**, *57*, 2499.

(34) Johnson, M. L.; Frasier, S. G. *Methods Enzymol.* **1985**, *117*, 301.

(35) Lakowicz, J. R.; Gratton, E.; Laczko, G.; Cherek, H.; Limkeman, M. *Biophys. J.* **1984**, *46*, 463.

(36) Guarr, T.; McGuire, M.; Strauch, S.; McLendon, G. *J. Am. Chem. Soc.* **1983**, *105*, 616.

(37) Murov, S. L.; Carmichael, I.; Hug, G. L. *Handbook of Photochemistry*, 2nd ed.; Marcel Dekker: New York, 1993.

(38) Typical diffusion coefficients calculated from the Stokes–Einstein relationship are typically on the order of 10^{-5} cm² s⁻¹ for small molecules in solutions of low viscosity. See ref 31.